

Superconducting Vortex Logic Antidots

C. J. Olson Reichhardt^{1,4}, C. Reichhardt^{2,4}, and B. Jankó^{3,4}

¹*T-12 and* ²*Center for Nonlinear Studies, Los Alamos National Laboratory, Los Alamos, New Mexico 87545*

³*Department of Physics, University of Notre Dame, Notre Dame, Indiana 46617*

⁴*Materials Science Division, Argonne National Laboratory, Argonne, Illinois 60429*

(February 7, 2020)

We examine a building block for logic devices in which the positions of superconducting vortices in coupled elongated antidots provide the elementary logic states of 0 and 1. We show analytically and through simulation the maximum operating frequency of a pair of antidots as a function of antidot spacing and elongation. At finite temperatures, a signal can propagate through a series of identically shaped antidots with correctly chosen spacing, with an exponential distribution of switching times for the signal to move over by one antidot.

PACS: 74.25.Qt,74.25.Sv

Recently there has been considerable interest in superconductors with artificial pinning arrays, such as artificial arrays of holes in thin-film type-II superconductors [1–3]. Under a magnetic field, the flux penetrates the film in the form of individual quantized vortices which become pinned by the holes. Experiments [1,2] and simulations [3] have shown that for fields where the number of vortices equals an integer multiple of the number of holes, peaks or anomalies in the transport and critical current occur. These anomalies are correlated with the formation of highly ordered vortex lattice crystals. Effective periodic pinning arrays can also be constructed by placing magnetic dots on superconductors, which produces strong pinning and commensuration effects [4], or by fabricating large “blind” holes (or antidots) which do not pass completely through the film but instead modulate the film thickness. In this case multiple vortices can be trapped at an individual antidot [5] and the vortex positions from one antidot are correlated with the positions in neighboring antidots [6]. Recently experiments have also demonstrated that nanodots of superconducting materials can capture individual vortices [7,8]. Besides circular pinning sites, it is also possible to fabricate elongated pinning sites [9]. In this case an individual vortex may not necessarily be located at the center of the pinning site but will reside along a line that cuts through the center of the site in the long direction.

Since the vortices have specific arrangements at certain integer matching or fractional matching fields, it should be possible to use the locations of the vortices or the flux configurations as elementary logic states such as 0 and 1. These states can then be measured or propagated by the application of a magnetic field or current. Puig *et al.* [10] made one initial proposal along these lines, in which a superconducting island with 2×2 plaquettes was considered as a logic element. In this case the minima in the resistance can be associated with different flux configurations.

The quantum-dot cellular automata (QCA) is another system that uses the locations or configurations of the particles as basic logic states [11,12]. A basic cell consists of four quantum dots containing two localized electrons. Due to the Coulomb repulsion between the electrons, there are two possible ground state configurations with the electrons located at the diagonals of the cell, slanted toward the right or left. These two states provide the fundamental logic units. With different geometrical arrangements of the basic cell, various logic devices can be constructed. In the QCA system the logic states are propagated by quantum-mechanical means. So far, elementary QCA systems have been demonstrated to operate only at extremely low temperatures. Since these systems must be adiabatically switched between logic states, signal propagation times are relatively slow.

In this paper we examine the building blocks for a superconducting vortex logic system [13] proposed in analogy with the quantum cellular automata. In our model we consider a superconductor that has been nanofabricated to contain elongated pinning sites, where each site captures a single vortex. Our basic unit consists of coupled elongated antidots of identical shape where, due to the repulsion of the vortices, two ground states can be formed. We show that by flipping one vortex in a pair of antidots, the vortex in the other antidot also flips, and we examine the response time of the second vortex as a function of the antidot geometry. We show that at finite temperatures, a signal can be propagated through a series of identically shaped antidots that have been fabricated in a specific geometry.

The individual logic element in our system is a single vortex inside an elongated antidot, a pinning site created through nanolithography techniques. As illustrated in Fig. 1(a), we take the elongation to be in the y direction. In the presence of a neighboring antidot, parallel to the first antidot and offset in the x direction, the two equilibrium positions of the vortex are at either end of

the antidot. Thus, to create our logic element, we define a vortex position at the top of the antidot to be a logic '1', as shown in Fig. 1(a), while a vortex positioned at the bottom of the antidot is in a logic '0' state. One way in which the logic state of the antidot can be externally controlled is by means of an STM tip made of magnetic material. If this tip is moved in the y direction at a given frequency, it should be possible to drag the vortex in the antidot below between the logic '0' and '1' states. The position of a vortex in a given antidot can also be detected by using an STM in spectroscopy mode. The vortex location can be identified due to the fact that the spectrum at the vortex core is very different from both superconducting or normal spectra [14].

In order to transmit information through the system, neighboring antidots must be coupled. We first consider an isolated pair of antidots a distance a apart, illustrated in Fig. 1(b). The vortices are prepared in an equilibrium configuration where vortex A is in logic state 1, and vortex B is in logic state 0. At time $t = t_0$ the position of vortex A is flipped by external means to be in logic state 0. For operation of the vortex logic, we require that vortex B will subsequently flip without external intervention to logic state 1, so that the final state of the system is reversed from the initial state.

In the case of two isolated antidots, vortex B does not need to overcome an energy barrier in order to flip. We can estimate the operating frequency of the two-vortex system by finding the time required to complete the flip. The interaction between the two vortices in a thin film is given by the Pearl interaction [15], which can be written

$$f^{vv}(r) = \frac{\Phi_0^2}{2\mu_0\pi\lambda^2} \frac{d}{r} \quad (1)$$

in the limit $r \ll 2\lambda^2/d$. Here, Φ_0 is the elementary flux quantum, μ_0 is the permeability of free space, λ is the London penetration depth of the superconductor, and d is the thickness of the superconducting film. The vortices obey overdamped dynamics given by $\mathbf{f}_i = \eta\mathbf{v}_i$, where $\eta = B_{c2}\Phi_0/\rho_N$, B_{c2} is the upper critical field, and ρ_N is the normal state resistivity. We assume that the antidots are spaced a apart in the x direction, and are of length α in the elongated y direction. If the position of vortex A is switched and held fixed such that both vortices are in the same logic state, vortex B requires a transit time t_{tr} before it reaches the opposite side of the antidot and the system returns to equilibrium. The transit time can be written

$$t_{tr} = \int_{\delta}^{\alpha} \frac{1}{v(y)} dy \quad (2)$$

where $v(y) = \mathbf{f} \cdot \hat{y}/\eta$, the y velocity of vortex B at position y . The integration must start from a small offset δ because if the two vortices are at the same y location, they exert no force on each other in the y direction and will

not move without thermal assistance. This means that in an experiment conducted at low temperatures where thermal fluctuations are insignificant, vortex A must be moved past the y position of vortex B by a distance δ . Putting in the approximation for the thin film interaction gives

$$\frac{t_{tr}}{t_0} = \frac{1}{2}(\alpha^2 - \delta^2) + a^2 \ln\left(\frac{\alpha}{\delta}\right) \quad (3)$$

where time is measured in units of $t_0 = \eta/f'_0$, with $f'_0 = \Phi_0^2/(2\pi\mu_0\lambda^2)$. Distances are measured in units of the film thickness d . Thus decreasing the spacing a or the antidot length α will produce faster switching.

We compare this theoretical result to the transit times of the vortex obtained from a two-dimensional numerical simulation with open boundary conditions. The equation of motion for a vortex i is

$$\mathbf{f}_i = \eta\mathbf{v}_i = \mathbf{f}_i^{vv} + \mathbf{f}_i^p + \mathbf{f}_i^T \quad (4)$$

The Langevin force from the temperature is \mathbf{f}_i^T and has the properties $\langle f^T(t) \rangle = 0$ and $\langle f_i^T(t)f_j^T(t') \rangle = 2\eta k_B T \delta_{ij} \delta(t - t')$. Initially we consider the case $T = 0$. The force \mathbf{f}_i^p is from the pinning well, represented by an ordinary parabolic trap that has been split in half and elongated in the y direction. There is no y direction confining force in the central elongated portion of the pin. The maximum pinning force is f_p in both the x and y directions. The radius of the pin is r_p , and the total length of the pin in the y direction is $\alpha + 2r_p$. We first consider two wells a distance a apart, each containing a single vortex.

Figure 2(a) shows the transit time t_{tr}/t_0 obtained from simulation (symbols) as a function of a with $T = 0$, $r_p = 0.24\lambda$, $f_p = 0.4f'_0$, $\delta = 0.24\lambda$, and $\alpha/\lambda = 3, 4, 5, \text{ and } 6$, along with corresponding plots of Eq. 3 (solid lines). In Fig. 2(b) we show t_{tr}/t_0 as a function of α for $a/\lambda = 3, 4, 5, \text{ and } 6$. In each case we find excellent agreement between simulation and theory. In the case of a Nb film of thickness 2000 Å with antidots of anisotropy $\alpha = 3\lambda = 135$ nm, and with spacing between the dots $a = 3\lambda = 135$ nm, the transit time of $t_{tr} = 27.2t_0$ from Eq. 3 with $\delta = 0.24\lambda = 10.8$ nm corresponds to an actual time of 1.4 ns, indicating that the maximum operating frequency for Nb antidots of this size and geometry is 696 MHz. Smaller or more closely spaced dots will operate at higher frequencies.

To create any type of device, the logic states need to be propagated over distances further than a single well. We therefore consider the case of three antidots, A, B, and C, illustrated in Fig. 1(c). All of the antidots are the same shape and size, but the antidot spacing varies, so that antidots A and B are separated by a , but antidots B and C are separated by a' . If $a' = a$, then when the vortex in dot A is switched externally, vortex B will not be able to switch because it experiences a potential barrier due

to the presence of vortex C. Instead, the new minimum energy for vortex B will be at the center of well B. This is undesirable for logic operations. In order to allow vortex B to switch, we must increase $a' > a$ to reduce the energy barrier produced by the repulsion from vortex C, and we must also introduce thermal fluctuations to allow thermal activation over the energy barrier. In a low-temperature material such as Nb, the thermal fluctuations may remain prohibitively small below T_c unless very small antidots are fabricated. In a high-temperature superconductor such as BSCCO, it is much easier to produce thermal activation even for relatively large antidots.

For the configuration shown in Fig. 1(c), where vortex A has been switched to a new logic state but vortex B has not yet switched, we can write an expression for the y position of vortex B at which the net y force on vortex B from vortices A and C is zero. We rescale all distances by α , so that $\tilde{y} = y/\alpha$, $\tilde{a} = a/\alpha$, and $\tilde{a}' = a'/\alpha$, and we take $\tilde{y} = 0$ as the starting position of vortex B and $\tilde{y} = 1$ as the final switched position. We obtain

$$2\tilde{y}_B^3 - 3\tilde{y}_B^2 + (1 + \tilde{a}'^2 + \tilde{a}^2)\tilde{y}_B - \tilde{a}^2 = 0. \quad (5)$$

After vortex B reaches \tilde{y}_B satisfying this expression, it has crossed the potential barrier and can move freely to the opposite side of the well. Similarly, after vortex B has switched to the new logic state [Fig. 1(d)], we can write an expression for the y position at which the force on vortex C from vortices A and B in the switched state is zero:

$$2\tilde{y}_C^3 - 3\tilde{y}_C^2 + (1 + \tilde{a}'^2 + 2\tilde{a}\tilde{a}' + 2\tilde{a}^2)\tilde{y}_C - \tilde{a}'^2 = 0. \quad (6)$$

The position \tilde{y}_C marks the end of the potential energy barrier.

Vortices B and C can cross their respective energy barriers by thermal activation. Well C should be placed as close as possible to well B in order to enhance the coupling of vortex C to vortex B, so a' should be made as small as possible. However, as a' approaches a , the coupling between vortices A and B is weakened, and vortex B will never switch initially. Thus a' should be chosen just slightly larger than the value at which vortex B can no longer switch. For $\tilde{a} = 0.187$, vortex B ceases to switch below $\tilde{a}'_{crit} = 0.29$; thus, for optimal operation, \tilde{a}' should be chosen slightly above \tilde{a}'_{crit} .

The thermal fluctuations must be large enough for vortices B and C to reach positions \tilde{y}_B and \tilde{y}_C at \tilde{a}'_{crit} by thermal activation in order for the signal to propagate. The vortices also thermally fluctuate in the x direction, and therefore if the antidots are wide in the x direction, the value of \tilde{a}'_{crit} is increased compared to the value obtained from Eqn. 5 since the minimum possible x distance a'_{eff} between vortices B and C is less than a' . The following relation holds: $a' - 2r_p < a'_{eff} < a'$. The same is true of a . Thus in experiments the pins must be fabricated slightly further than a or a' apart. Additionally,

since the switching of the vortices is now thermally activated, strict clocking of the signal is *no longer possible* as it was in the case of two wells. A mechanism to obtain strict clocking has been demonstrated in Ref. [13].

The distance between the wells required for the operation of the three well system scales with α . The smaller α is, the smaller the distance between pins can be made and still allow operation of all three wells. We consider the case of BSCCO where thermal activation can play a significant role below T_c . In Fig. 3 we show the distribution of switching times $P(t_s)$ obtained from 200 runs with different random temperature seeds. Here $f_T = 1.2f'_0$, $a = 0.5\lambda$, $a' = 0.68\lambda$, and $\alpha = 2.48$. Fig. 3(a) shows that $P(t_s^{(B)})$ for vortex B is exponentially distributed with mean value $\bar{t}_s^{(B)} = 1078t_0$. $P(t_s^{(C)})$ for vortex C, with time measured from $t = 0$ before vortex B has switched, is plotted in Fig. 3(b), and the distribution is clearly broader and more heavily weighted toward later times. $P(t_s^{(C)})$ for vortex C is merely the product of two exponential distributions, as can be seen from Fig. 3(c), where we plot the switching time of vortex C with time measured from $t = t_s^{(B)}$, the switching time of vortex B. $P(t_s^{(C)} - t_s^{(B)})$ is also exponentially distributed with a mean value of $693t_0$.

More than three wells can be connected, but the spacing between well n and $n + 1$ must always be greater than the spacing between wells n and $n - 1$. Thus there is a practical limitation on the total length of device that can be fabricated in this fashion; when the wells are spaced too far apart, the vortices will thermally decouple. Additionally, as illustrated in Fig. 3, the distribution of switching times for the final well will become increasingly broad and approach a Gaussian as the number of wells is increased. Regardless of the number of wells, these logic elements operate only from the narrowly spaced end to the widely spaced end. A signal introduced at the widely spaced end will not be able to propagate to the narrow end. If all the wells are spaced equally, it is still possible for excitations to propagate through the wells under thermal activation if the temperature is high enough. However, these excitations move diffusively in either direction and are not well controlled. It is possible instead to employ a ratchet mechanism to obtain controlled, clocked motion of the signal [13].

In summary we have examined the basic building blocks for a vortex cellular automata that is analogous to a quantum-dot cellular automata. We consider elongated pinning sites in superconducting samples where there is one vortex per antidot. The vortices can form two ground states with the vortices located at diagonals in order to minimize their interaction energy. We obtained analytically and in simulation the maximum frequency of operation for a two well system. For the simplest pipeline geometry of three wells we find that, for finite temperatures, a change in logic state introduced at the first well

can be propagated over specified distances.

Acknowledgments— We thank W. Kwok and V.V. Metlushko for useful discussions. This work was supported by the U.S. DoE, Office of Science, under Contract No. W-31-109-ENG-38. CJOR and CR were supported by the U.S. DoE under Contract No. W-7405-ENG-36. BJ was supported by NSF-NIRT award DMR02-10519. and the Alfred P. Sloan Foundation.

-
- [1] A.T. Fiory, A.F. Hebard, and S. Somekh, *Appl. Phys. Lett.* **32**, 73 (1978).
[2] M. Baert, V.V. Metlushko, R. Jonckheere, V.V. Moshchalkov, and Y. Bruynseraede, *Phys. Rev. Lett.* **74**, 3269 (1995); K. Harada, O. Kamimura, H. Kasai, F. Matsuda, A. Tonomura, and V.V. Moshchalkov, *Science* **274**, 1167 (1996); S.B. Field, S.S. James, J. Barentine, V. Metlushko, G. Crabtree, H. Shtrikman, B. Ilic, and S.R.J. Brueck, *Phys. Rev. Lett.* **88**, 067003 (2002).
[3] C. Reichhardt, C.J. Olson and F. Nori, *Phys. Rev. Lett.* **78**, 2648 (1997).
[4] J.I. Martín, M. Vélez, J. Nogues, and I.K. Schuller, *Phys. Rev. Lett.* **79**, 1929 (1997); D.J. Morgan and J.B. Ketterson, *Phys. Rev. Lett.* **80**, 3614 (1998); J.I. Martín, M. Vélez, A. Hoffmann, I.K. Schuller, and J.L. Vicent, *Phys. Rev. Lett.* **83**, 1022 (1999); A. Terentiev, D.B. Watkins, L.E. De Long, L.D. Cooley, D.J. Morgan, and J.B. Ketterson, *Phys. Rev. B* **61**, R9249 (2000).
[5] A. Bezryadin, Y.N. Ovchinnikov, and B. Pannetier, *Phys. Rev. B* **53**, 8553 (1996)
[6] C. Reichhardt and N. Grønbech-Jensen, *Phys. Rev. Lett.* **85**, 2372 (2000).
[7] A.K. Geim, I.V. Grigorieva, S.V. Dubonos, J.G.S. Lok, J.C. Maan, A.E. Filippov, and F.M. Peeters, *Nature (London)* **390**, 259 (1997).
[8] P.S. Deo, V.A. Schweigert, F.M. Peeters, and A.K. Geim, *Phys. Rev. Lett.* **79**, 4653 (1997); V.A. Schweigert, F.M. Peeters, and P.S. Deo, *Phys. Rev. Lett.* **81**, 2783 (1998); K. Tanaka, I. Robel, and B. Jánko, *Proc. Nat. Acad. Sci.* **99**, 5233 (2002).
[9] V.V. Metlushko *et al.* (unpublished).
[10] T. Puig, E. Rosseel, M. Baert, M.J. Van Bael, V.V. Moshchalkov, and Y. Bruynseraede, *Appl. Phys. Lett.* **70**, 3155 (1997).
[11] C.S. Lent, P.D. Tougaw, W. Porod, and G.H. Bernstein, *Nanotechnology* **4**, 49 (1993).
[12] I. Amlani, A.O. Orlov, G. Toth, G.H. Bernstein, C.S. Lent, and G.L. Snider, *Science* **284**, 289 (1999).
[13] M.B. Hastings, C.J. Olson Reichhardt, and C. Reichhardt, *Phys. Rev. Lett.* **90**, 247004 (2003).
[14] H.F. Hess, R.B. Robinson, and J.V. Waszczak, *Phys. Rev. Lett.* **64**, 2711 (1990); S.H. Pan, E.W. Hudson, A.K. Gupta, K.-W. Ng, H. Eisaki, S. Uchida, and J.C. Davis, *ibid.* **85**, 1536 (2000).
[15] J.R. Clem, *Phys. Rev. B* **43**, 7837 (1991).

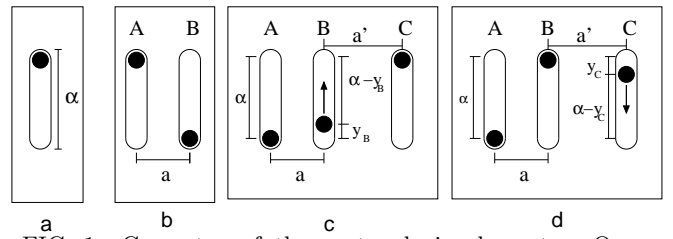


FIG. 1. Geometry of the vortex logic elements. Open shapes represent the antidots, and filled circles represent the vortices. (a) A single antidot of elongation α . The vortex is shown in logic state 1, at the top of the antidot. Logic state 0 is represented when the vortex is at the bottom of the antidot. (b) Vortices A and B in neighboring antidots separated by distance a assume opposite logic states. (c) An example of a signal propagating through three antidots. Vortex A has been switched to logic state 0. Vortex B is in the process of switching, and has moved a distance y_B . The spacing between antidots A and B is a , and the spacing between antidots B and C is $a' > a$. (d) Vortex C is in the process of switching, and has moved a distance y_C .

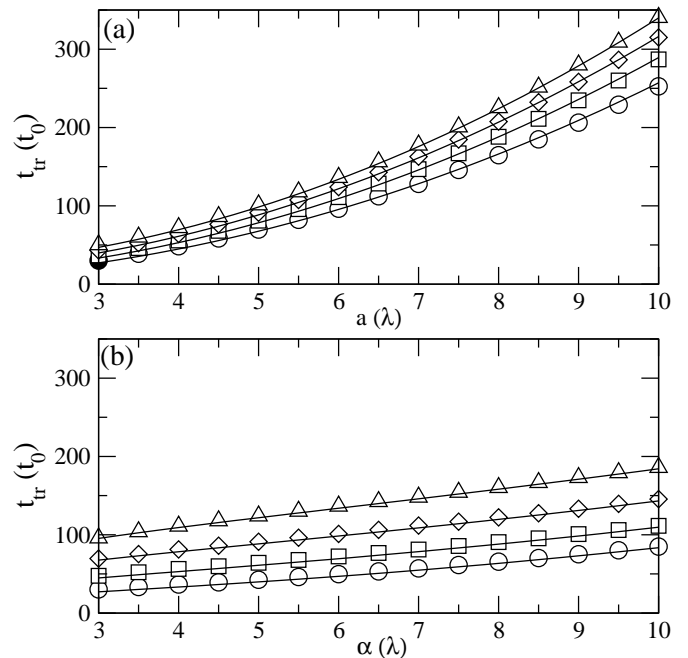


FIG. 2. Transit time t_{tr} for vortex B to cross the antidot and move from one logic state to the other after vortex A has been switched. (a) t_{tr} as a function of antidot spacing a for fixed $\alpha = 3$ (circles), 4 (squares), 5 (diamonds), and 6 (triangles), for a two-well system with $T = 0$, $r_p = 0.24\lambda$, $f_p = 0.4f'_0$, and $\delta = 0.24\lambda$. The symbols represent transit times measured in simulations, while the lines are plots of Eq. 3. (b) t_{tr} from simulation and Eq. 3 for the same system as a function of antidot anisotropy α with fixed $a = 3$ (circles), 4 (squares), 5 (diamonds), and 6 (triangles).

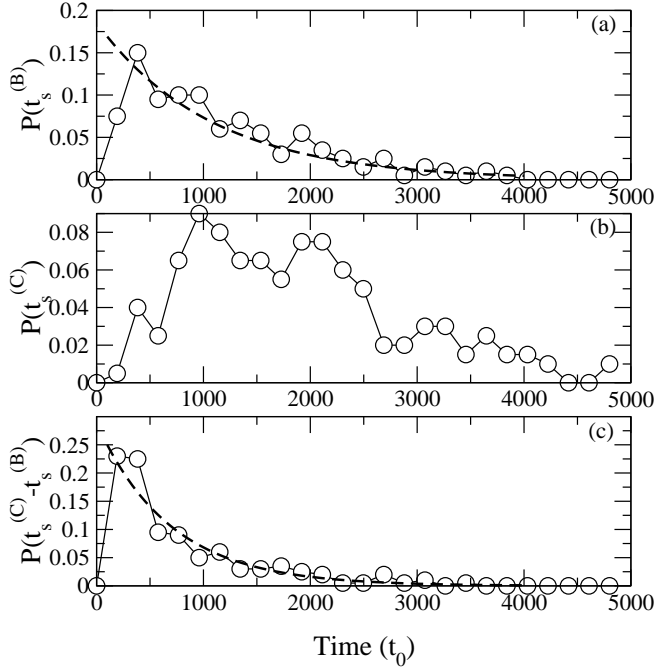


FIG. 3. (a) The distribution of switching times $P(t_s^{(B)})$ for vortex B obtained from 200 independent simulations of a system with $f_T = 1.2f'_0$, $a = 0.5\lambda$, $a' = 0.68\lambda$, and $\alpha = 2.48$. Time is measured from $t = 0$. The dashed line indicates an exponential distribution with parameter $1/\lambda_e = 1078t_0$, the mean value $\bar{t}_s^{(B)}$. (b) $P(t_s^{(C)})$ for vortex C, with time measured from $t = 0$. The mean switching time is $\bar{t}_s^{(C)} = 1771t_0$. (c) $P(t_s^{(C)} - t_s^{(B)})$ for vortex C, with time measured from $t = t_s^{(B)}$ for each run, the time at which vortex B switched. The dashed line indicates an exponential distribution with parameter $1/\lambda_e = 693t_0$, which is $\bar{t}_s^{(C)} - \bar{t}_s^{(B)}$.